P2.9 CONVERSION OF NARROWBAND VISIBLE RADIANCES TO BROADBAND SHORTWAVE RADIANCES USING COINCIDENT CERES AND VIRS DATA

Venkatesan Chakrapani, David R. Doelling,
AS&M, Inc., Hampton, VA 23666 USA

Patrick Minnis
NASA-Langley Research Center

1. INTRODUCTION

Monitoring of the top of atmosphere regional radiation budgets is limited by the availability of broadband measurement systems. However, the Earth Radiation Budget Experiment (ERBE) and the recent Clouds and the Earth's Radiant Energy System (CERES) provide a limited temporal dataset. If all the operational geostationary and polar satellites had broadband capabilities, this would provide a more complete dataset. Current plans call for the placement of the Geostationary Earth Radiation Budget GERB broadband instrument on the Meteosat Second Generation Satellite (MSG). However it is unlikely that all future satellites will have broadband instruments. A potential solution for this problem is the conversion of narrowband data into broadband fluxes. As shown by Young et al. (1998), incorporation of geostationary satellite data would greatly reduce errors due to temporal sampling and are being utilized in the time-space averaged products for CERES. Narrowband-to-broadband conversions that do not involve computer intensive radiative transfer models or those that do not require large apriori data set would be ideal for use on an operational basis.

The narrowband-to-broadband models currently used in the Atmospheric Radiation Measurement (ARM) program geostationary products involve narrowband-to-broadband shortwave albedo conversions. Conversion formulas based on regressions of narrowband and broadband albedos that include a solar zenith angle term and have a 10% relative RMS error (Doelling et al. 1999). The errors in this approach result from the lack of terms accounting for cloud properties, vegetation cycles, and from inaccurate bidirectional models. The greatest error occurs in cloudy conditions.

The CERES Single Scanner Footprint TOA/Surface and Clouds (SSF) dataset provides coincident, collocated and co-angled broadband shortwave and narrowband visible data. This paper uses CERES data from the Tropical Rainfall Measuring Mission (*TRMM*) satellite to derive angular based narrow-to-broadband radiance models. The conversions are modeled as functions of angles, and geo-type. Visible Infrared Scanner (VIRS) derived cloud optical depth and phase are also used to stratify cloudy scenes. Since the models are derived at the radiance level, they are independent of bidirectional model, any bidirectional model may be used to invert the radiances to fluxes. These models can then be applied to pixel level imager data that have similar visible spectral response functions, to compute more accurate high resolution broadband shortwave fluxes from VIS radiances.

*Corresponding author address: Venkatesan Chakrapani, AS&M, Inc., 1 Executive Pkwy, Hampton, VA 23666. email: v.chakrapani@larc.nasa.gov.

2. DATA

TRMM CERES SSF broadband shortwave (SW 0.3-5 μm) radiances, at a nominal 10-km footprint, are matched with VIRS imager visible (VIS 0.65μm) radiances and cloud properties that are contained in the CERES footprint (Minnis et al. 2002). The VIRS imager pixels, which have a nominal field of view of 2 km, are weighted by the CERES point-spread function in order to closely match the spatial radiance pattern seen by CERES. The CERES SSF cross-track dataset provides coincident, collocated, and co-angled narrowband and broadband radiances. The CERES *TRMM* data are available from January to August 1998. *TRMM* CERES operated in the cross-track scan mode 2 out of every 3 days for a total of 192 days. The VIRS dataset is limited to a 45° viewing zenith angle, due to the scan limit of the VIRS instrument and to ±37° latitude because of the *TRMM* satellite orbit. The *TRMM* orbit precesses every 48 days and samples all local hours in 24 days. This orbit assures that solar zenith angle variations are not geographically dependent, as is the case with polar orbiters.

The radiances are grouped in a similar manner as the CERES bidirectional reflectance models (Loeb et al. 2002). The CERES models use the Rotating Azimuth Plane Scan (RAPS) mode data to retrieve all view angles and to increase regional bin sampling. The data are grouped by angles as follows: 9 solar zenith angle bins, one every 10°; 5 view angle bins, one every 10°, and 10 relative azimuthal angle bins, one every 20° except for 10° in the forward and backscatter bins. The radiances are further grouped into 5 geo-types that are classified by International Geosphere – Biosphere Program (IGBP) type. The IGBP land types were sorted by albedo into 4 groups, forest, grasslands, dark and

bright deserts. The remaining geo-type is ocean. VIRS derived cloud properties (Minnis et al. 2002) are used to further group the cloudy scenes into either water or ice clouds. In order for the CERES footprint to be considered, 90% of the VIRS pixels must be either clear, water, or ice cloud. Usually operational satellite imager pixels are either classified as clear or cloudy. The cloudy footprints are further subdivided into 6 optical depth bins bounded by; 0.01, 2.5, 6, 10, 18, 40, and >40. There was sufficient sampling for most bins, some clear ocean bins have over 100,000 pixels, with the exception of all scenes at low sun angles in the forward and backscatter conditions. Also, many cloud categories over deserts are missing. A bin must contain at least 100 pixels to be used in the model.

3. RESULTS

The first step is to derive a partial bidirectional model for both the narrowband and broadband radiances. The term partial is used here to denote that the model lacks view zenith angles greater than 45°. No attempt is made to model them. The bidirectional reflectance factor is simply the bin reflectance divided by the albedo for a given solar zenith angle. The partial albedo is computed by summing the available bin radiances weighted by the squared sine of the view angle and width of the azimuth bin. The partial albedo may be lower than the true albedo generated with a complete set of viewing angles. Figure 1 shows the bidirectional factors for clear ocean for the narrowband and broadband at a solar zenith angle of 35°. The left half of the plot contains the forward scattering bins and the right half contains the backscatter. The narrowband is more anisotropic than the broadband under glint conditions. The narrowband albedo is 0.076 and the broadband is 0.080. The narrowband to broadband (NB-BB) ratio, 0.956, is defined as the narrowband divided by the broadband. Figure1c shows the radiance-level NB-BB ratio, which is computed in terms of reflectance to remove the effects of the solar constant differences. For the figures in this paper, all the bin ratios are then normalized to the partial albedo ratio with the ratio given on the left side of the plot. One can then easily compare the angular variation of the relative ratio differences between scenes, although the albedo ratio may be quite different. For clear ocean, at 35° solar zenith angle, there is more reflection in the broadband. However in the forward scattering angles where the relative ratio is greater than 1.05 the narrowband is more reflective than broadband. There is broadband absorption in the glint area than for shorter wavelengths.

The ratios for clear land types for 35° solar zenith angle are shown in Fig. 2. Clear ocean has the greatest angular variation in the NB-BB ratio; however, forest has the greatest difference between the narrowband and broadband albedos. This is due to increased near-IR reflection of vegetation, especially lush green forests. The overall ratio for forest is 0.743, 0.845 for grass, 1.014 for dark desert and 1.125 for bright deserts. Deserts have little or no vegetation and the higher desert albedos increase the absorption in the broadband, which is not the case in the narrowband window. The mean clear broadband albedos are 0.15, 0.17, 0.20, 0.27 for forest, land, dark and bright deserts, respectively. The angular features decrease as the vegetation diminishes. For bright deserts, the angular variation is less than 4%. For all land scenes the narrowband and broadband bidirectional models have similar features. The current model does account for regional vegetation variations within similar IGBP types or the vegetation seasonal cycle. NB- BB models based on the *Terra* CERES SSF product, should be able to resolve the vegetation variations, since the *Terra* satellite contains the MODIS imager, which has a vegetation channel (0.86 μm).

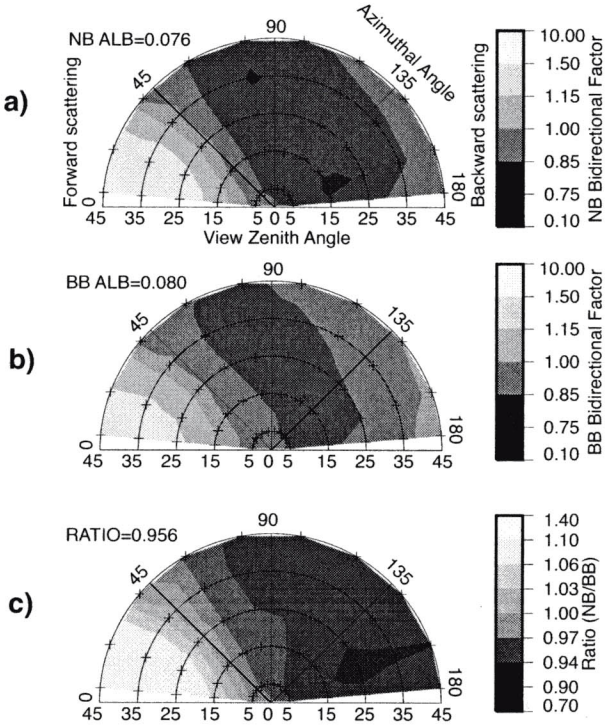

Fig. 1 Clear ocean bidirectional factors for a) narrowband and b) broadband at a solar zenith angle of 35°. View angle is given on the bottom of each plot and azimuth angle varies radially, where 0° is in the forward scattering direction. The matching NB-BB ratio is displayed in c). The corresponding partial albedo or NB-BB albedo ratio is noted in the left-hand top corner.

The NB-BB ratio angular variation of ice and water clouds over forest for two optical depths is shown in Fig. 3. Optically thick clouds have little angular variation, are independent of underlying geo-type, and the angular variation is consistent between geo-types. Both ice and water clouds appear fairly Lambertian in the broadband as well as in the narrowband spectrum. Optically thin clouds over forest have similar but less distinct angular

features compared to those for clear conditions. For ocean, only the first optical depth bin (τ<2.5) retains some clear-sky features. For increasing optical depth the NB-BB albedo ratio increases.

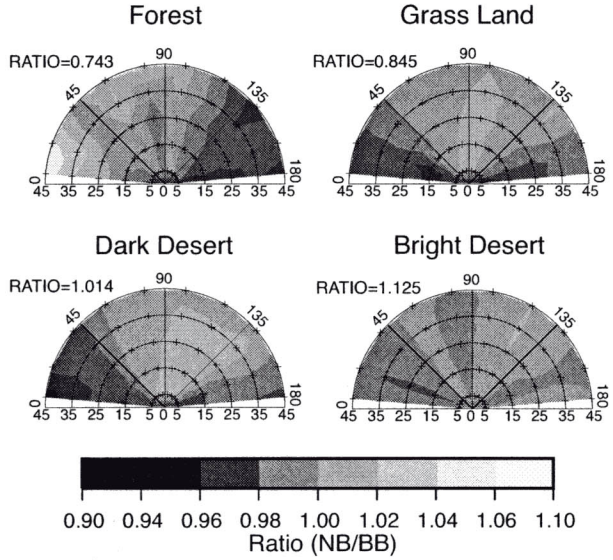

Fig. 2. The NB-BB ratio for forest, grass, dark and bright desert under clear-sky conditions at a solar zenith angle of 35°. The axis values are the same as in Fig. 1.

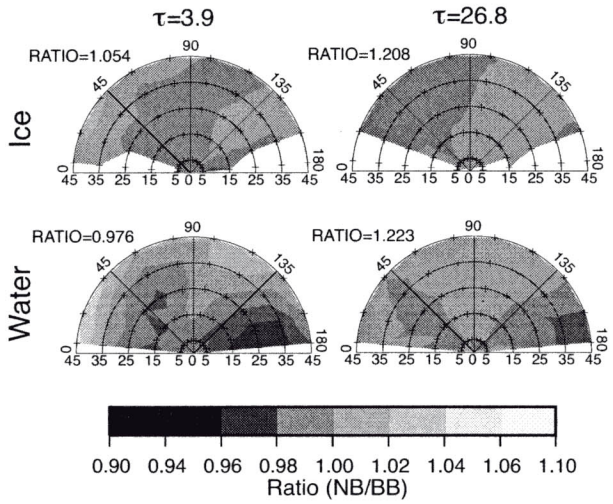

Fig. 3. The NB-BB ratio for ice clouds (top row) and water clouds (bottom row) and optical depth bins centered at 3.9 (left column) and 26.8 (right column) over forest. The axis values are the same as in Fig. 1.

Partial albedos are computed for all scenes and solar zenith angles. The partial directional models are generally more flat with respect to solar zenith angle than if all viewing angles are available. In Fig. 4a the partial albedos at solar zenith angle of 35° over ocean of both narrowband and broadband water and ice clouds are shown. In general, ice clouds are brighter than water clouds. Similar parameters over forest are shown in Fig. 5a. The ocean NB-BB albedo ratio increases from near unity in clear conditions to 1.2 for optically thick clouds (see Fig. 4b). Both ice and water clouds have approximately the same NB-BB ratio. Over forest, the narrowband albedo is less than the broadband albedo for optically thin clouds, which is not the case for ocean conditions. Ice clouds over forest have a greater NB-BB albedo ratio for optically thin clouds than those over oceans. However, for large optical depths, the ratios are similar.

4. CONCLUSIONS

An angular radiance NB-BB ratio model was developed to more accurately convert narrowband radiances into broadband radiances compared to simple empirical albedo models. The NB-BB ratio models also account for cloud optical depth and phase. Clear scenes have more angular NB-BB ratio features than do cloudy scenes. The same holds true for vegetated as compared to non-vegetated land types. Clear ocean glint conditions have greater partial narrowband albedo than broadband albedo. Ratios for optically thick clouds are independent of underlying geo-type. Optically thick clouds have greater narrowband than broadband albedos. Lush vegetation has a greater broadband albedo than narrowband. As vegetation diminishes, the narrowband albedo becomes more similar to the broadband albedo. For bright deserts the narrowband albedo is greater than the broadband albedo.

5. FUTURE WORK

This NB-BB ratio model will be validated using the *TRMM* CERES SSF Rotating Azimuth Plane Scan (RAPS) fluxes with coincident cross-track VIRS-derived broadband fluxes. The coincident VIRS and CERES pixels have differing viewing geometries. The NB-BB ratio model will then be applied to the VIRS reflectances and then the CERES bidirectional model is used to convert the radiance to flux. The narrowband derived broadband fluxes will then be compared with the CERES fluxes.

The NB-BB ratio model will also be validated using GOES imager data and coincident CERES fluxes. This requires cross-calibration between GOES-8 and VIRS imager radiances to take into account calibration and spectral response function differences.

REFERENCES

Doelling D. R. et al., 1999: Broadband radiation fluxes from narrowband fluxes. Proceedings of the ALPS-99 conference. Meribel, France, January 18-22, Wk-P-16,1-5

Loeb, N. G. et al., 2002: A new generation of angular distribution models for top-of-atmosphere radiative flux estimation from the Clouds and Earth's Radiant Energy System (CERES) satellite instrument. *AMS*

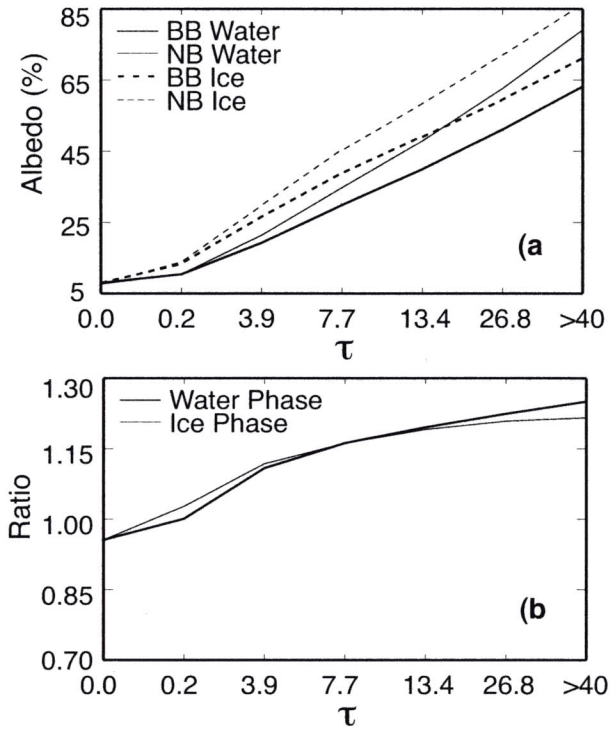

Fig. 4. a) The partial albedo for water and ice clouds for both narrowband and broadband channels as a function cloud optical depth for ocean. The 0 optical depth value represents clear-sky conditions. b) The NB-BB albedo ratio for ice and water clouds

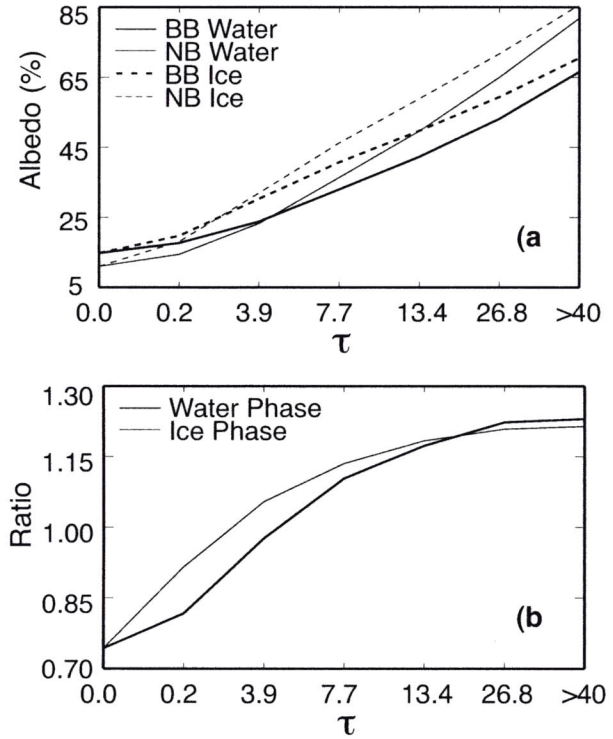

Fig. 5. Same as Fig. 4. except for forest.

11th Conference on Atmospheric Radiation, Ogden, Utah, June 3-7.

Minnis, P., W. L. Smith, Jr., and D. F. Young, 2001: Cloud macro- and microphysical properties derived from GOES over the ARM SGP domain. *Proceedings of the ARM 11th Science Team Meeting*, Atlanta, GA, March 19-23, 11 pp. (available at http://www.arm.gov/docs/ documents/technical/conf_0103/minnis-p.pdf).

Minnis, P., D. F .Young, B. A. Wielicki, D. P. Kratz, P. W. Heck, S. Sun-Mack, Q. Z. Trepte, Y. Chen, S. L. Gibson, R. R. Brown, 2002: Seasonal and diurnal variations of cloud properties derived for CERES from VIRS and MODIS data. *Proc. 11th AMS Conf. Atmos. Rad.*, Ogden, UT, June 3-7.

D. F. Young, P. Minnis, D. R. Doelling, G. G. Gibson, T. Wong, 1998: Temporal interpolation methods for the Clouds and Earth's Radiant Energy System (CERES) Experiment. *J. Appl. Meteorol.*, **37**, 572-590.